



**HAL**  
open science

## White-to-brite conversion in human adipocytes promotes metabolic reprogramming towards fatty acid anabolic and catabolic pathways

V Barquissau, D. Beuzelin, D. Pisani, G.E. Beranger, A. Mairal, Alexandra Montagner, B. Roussel, Geneviève Tavernier, Ma. Marques, C. Moro, et al.

### ► To cite this version:

V Barquissau, D. Beuzelin, D. Pisani, G.E. Beranger, A. Mairal, et al.. White-to-brite conversion in human adipocytes promotes metabolic reprogramming towards fatty acid anabolic and catabolic pathways. *Molecular metabolism*, 2016, 5 (5), pp.352-365. 10.1016/j.molmet.2016.03.002 . hal-02134884

**HAL Id: hal-02134884**

**<https://hal.science/hal-02134884>**

Submitted on 27 May 2020

**HAL** is a multi-disciplinary open access archive for the deposit and dissemination of scientific research documents, whether they are published or not. The documents may come from teaching and research institutions in France or abroad, or from public or private research centers.

L'archive ouverte pluridisciplinaire **HAL**, est destinée au dépôt et à la diffusion de documents scientifiques de niveau recherche, publiés ou non, émanant des établissements d'enseignement et de recherche français ou étrangers, des laboratoires publics ou privés.



Distributed under a Creative Commons Attribution - NonCommercial - NoDerivatives 4.0 International License



# White-to-brite conversion in human adipocytes promotes metabolic reprogramming towards fatty acid anabolic and catabolic pathways

V. Barquissau<sup>1,2,8</sup>, D. Beuzelin<sup>1,2,8</sup>, D.F. Pisani<sup>3,4,5</sup>, G.E. Beranger<sup>3,4,5</sup>, A. Mairal<sup>1,2</sup>, A. Montagner<sup>2,6</sup>, B. Roussel<sup>1,2</sup>, G. Tavernier<sup>1,2</sup>, M.-A. Marques<sup>1,2</sup>, C. Moro<sup>1,2</sup>, H. Guillou<sup>2,6</sup>, E.-Z. Amri<sup>3,4,5</sup>, D. Langin<sup>1,2,7,\*</sup>

## ABSTRACT

**Objective:** Fat depots with thermogenic activity have been identified in humans. In mice, the appearance of thermogenic adipocytes within white adipose depots (so-called brown-in-white *i.e.*, brite or beige adipocytes) protects from obesity and insulin resistance. Brite adipocytes may originate from direct conversion of white adipocytes. The purpose of this work was to characterize the metabolism of human brite adipocytes.

**Methods:** Human multipotent adipose-derived stem cells were differentiated into white adipocytes and then treated with peroxisome proliferator-activated receptor (PPAR) $\gamma$  or PPAR $\alpha$  agonists between day 14 and day 18. Gene expression profiling was determined using DNA microarrays and RT-qPCR. Variations of mRNA levels were confirmed in differentiated human preadipocytes from primary cultures. Fatty acid and glucose metabolism was investigated using radiolabelled tracers, Western blot analyses and assessment of oxygen consumption. Pyruvate dehydrogenase kinase 4 (PDK4) knockdown was achieved using siRNA. *In vivo*, wild type and PPAR $\alpha$ -null mice were treated with a  $\beta_3$ -adrenergic receptor agonist (CL316,243) to induce appearance of brite adipocytes in white fat depot. Determination of mRNA and protein levels was performed on inguinal white adipose tissue.

**Results:** PPAR agonists promote a conversion of white adipocytes into cells displaying a brite molecular pattern. This conversion is associated with transcriptional changes leading to major metabolic adaptations. Fatty acid anabolism *i.e.*, fatty acid esterification into triglycerides, and catabolism *i.e.*, lipolysis and fatty acid oxidation, are increased. Glucose utilization is redirected from oxidation towards glycerol-3-phosphate production for triglyceride synthesis. This metabolic shift is dependent on the activation of PDK4 through inactivation of the pyruvate dehydrogenase complex. *In vivo*, PDK4 expression is markedly induced in wild-type mice in response to CL316,243, while this increase is blunted in PPAR $\alpha$ -null mice displaying an impaired brite response.

**Conclusions:** Conversion of human white fat cells into brite adipocytes results in a major metabolic reprogramming inducing fatty acid anabolic and catabolic pathways. PDK4 redirects glucose from oxidation towards triglyceride synthesis and favors the use of fatty acids as energy source for uncoupling mitochondria.

© 2016 The Authors. Published by Elsevier GmbH. This is an open access article under the CC BY-NC-ND license (<http://creativecommons.org/licenses/by-nc-nd/4.0/>).

**Keywords** Brite/beige adipocyte; Peroxisome proliferator-activated receptor; Fatty acid metabolism; Glycerol metabolism; Pyruvate dehydrogenase kinase 4

## 1. INTRODUCTION

Obesity results from energy imbalance. When energy intake chronically exceeds energy expenditure, white adipose tissue (WAT) dramatically expands to store the excess of energy as fat. Brown adipose tissue (BAT) is responsible for the maintenance of body core temperature leading to energy expenditure. This thermogenic function of BAT relies on the activity of uncoupling protein 1 (UCP1), which dissociates substrate oxidation from ATP production [1]. In addition to its thermoregulatory function, UCP1 regulates whole-body energy

homeostasis as its ablation leads to obesity in mice housed at thermoneutrality [2]. Adult humans possess active BAT [3–5]. BAT activity is negatively associated with adiposity, insulin resistance and aging. Therefore, therapeutics aimed at increasing BAT recruitment and activity appear conceivable strategies to fight obesity and its metabolic complications [6].

Classical brown adipocytes are multilocular, UCP1-positive and thermogenically-competent cells residing in anatomically defined BAT depots. Following cold-exposure [7–9] or treatments with  $\beta_3$ -adrenergic receptor agonists [10–12], brown-like fat cells are detected in mouse

<sup>1</sup>INSERM, UMR 1048, Institute of Metabolic and Cardiovascular Diseases, Toulouse, France <sup>2</sup>University of Toulouse, Paul Sabatier University, France <sup>3</sup>University of Nice Sophia Antipolis, Nice, France <sup>4</sup>CNRS, iBV, UMR 7277, Nice, France <sup>5</sup>INSERM, iBV, U 1091, Nice, France <sup>6</sup>INRA, UMR 1331, TOXALIM, Toulouse, France <sup>7</sup>Toulouse University Hospitals, Laboratory of Clinical Biochemistry, Toulouse, France

<sup>8</sup>V. Barquissau and D. Beuzelin contributed equally to this work.

\*Corresponding author. UMR 1048, Institute of Metabolic and Cardiovascular Diseases, CHU Rangueil, 1 avenue Jean Poulhès, BP 84225, 31432 Toulouse Cedex 4, France. Tel.: +33 5 61 32 56 28; fax: +33 5 61 32 56 23. E-mail: [dominique.langin@inserm.fr](mailto:dominique.langin@inserm.fr) (D. Langin).

Received March 3, 2016 • Accepted March 13, 2016 • Available online 18 March 2016

<http://dx.doi.org/10.1016/j.molmet.2016.03.002>

subcutaneous inguinal WAT depot [13,14] where they are interspersed within unilocular UCP1-negative white adipocytes [15]. In mice, browning of WAT is associated with protection against high-fat diet-induced obesity and insulin resistance [16,17]. Brown-like adipocytes in WAT depots have been named brite (brown-in-white) or beige adipocytes. Two origins for brite adipocytes have been proposed. Brite fat cells may originate from *de novo* differentiation of precursor cells [18,19] or arise from direct conversion of mature white fat cells [7,20,21].

In humans, brite adipocytes have been observed in white fat depots [22,23]. Morphological and histological data revealing cells with an intermediate phenotype suggest that conversion of white into brite adipocytes likely occurs [22]. However, most studies investigating human brown/brite adipogenesis focused on differentiation of precursors into mature brown-like adipocytes [24–28]. Despite the therapeutic interest in the transformation of energy-storing into energy-dissipating adipocytes, data on fat and glucose metabolism during conversion from human white to brite fat cells are scarce. Notably, it is not established whether browning of white fat cells promotes both fatty acid and glucose utilization and how these changes are related to other metabolic pathways. Treatment with rosiglitazone, a PPAR $\gamma$ -specific agonist, of human multipotent adipose-derived stem (hMADS) cells previously differentiated into white adipocytes drives gene expression of brown/brite fat markers through the formation of PPAR $\gamma$  super-enhancers [29–31]. Long-term exposure to PPAR $\alpha$  agonist induces a thermogenic programme in murine subcutaneous WAT [32,33]. Furthermore, the two nuclear receptors are known positive regulators of UCP1 expression in mouse brown adipocytes [34,35].

In the present work, conversion of white hMADS adipocytes into brite fat cells was induced with selective PPAR $\gamma$  and PPAR $\alpha$  agonists to investigate fat and glucose metabolism. *In vivo*, subcutaneous WAT of wild type and PPAR $\alpha$ -null mice were analyzed following chronic  $\beta_3$ -adrenergic treatment.

## 2. MATERIALS AND METHODS

### 2.1. hMADS adipocytes

hMADS cells, established from the prepubic fat pad of a 4-month-old male (hMADS-3), were used between passages 16 and 25. hMADS cells were cultured and differentiated into white adipocytes as previously described [36]. At day 14, 100 nM of the PPAR $\gamma$  agonist, rosiglitazone (Rosi), or 300 nM of the PPAR $\alpha$  agonist, GW7647 (GW), were added to the differentiation medium for 4 additional days (Figure S1A). Agonists were selected for being specific of each human PPAR subtype [37,38]. Human fibroblast growth factor 2, insulin, triiodothyronine, transferrin, 3-isobutyl-1-methylxanthine, GW and dexamethasone were from Sigma; L-glutamine, penicillin, and streptomycin from Invitrogen; HEPES, low glucose Dulbecco's modified Eagle medium and Ham's F-12 medium from Lonza; Rosi from Alexis Biochemicals.

#### 2.1.1. Triglyceride content

Lipid accumulation was visualized by Oil Red O staining of 10% formalin-fixed differentiated cells. Colorimetric quantitation of triglyceride content was performed using the triglyceride reagent commercial kit (Sigma). Values were normalized to protein concentration in cell lysates.

#### 2.1.2. mRNA expression in hMADS cells

hMADS cells were harvested in RLT- $\beta$ -mercaptoethanol 1% from the RNA extraction kit (Qiagen). Total RNA was extracted using RNeasy mini kit (Qiagen) and quantified by Nanodrop spectrophotometer (ThermoFischer Scientific). RNA (500 ng–1  $\mu$ g) was reverse transcribed with the High capacity cDNA reverse transcription kit (Applied

Biosystems) and qPCR was performed on a StepOnePlus thermocycler (ThermoFischer Scientific) using Fast SYBR green or Taqman fast advanced master mixes (Life Technologies). SYBR Green primers (Eurogentec) and Taqman probes (Life Technologies) are listed in Tables S1 and S2. LRP10 was used as housekeeping gene.

#### 2.1.3. DNA microarray

Total RNA from control and Rosi- or GW-treated cells ( $n = 4$  for each condition) was extracted using a TRI-Reagent kit (Euromedex). RNA quality was checked by capillary electrophoresis (Experion, Bio-Rad). Microarray experiments were performed using Agilent 4  $\times$  44k v2 oligonucleotide arrays as previously described [39]. Microarray data have been deposited in NCBI's Gene Expression Omnibus and are accessible through GEO Series accession number GSE71293. Significant microarray analysis (SAM) was performed to determine differentially expressed genes in Rosi- or GW-treated cells compared to control cells at day 18. Biological pathways and processes were analyzed using DAVID database v6.7 with Benjamini correction of  $p$  values [40].

#### 2.1.4. Western blot

Cells were lysed in RIPA buffer (Sigma) containing cocktail of protease and phosphatase inhibitors (Sigma). Equal amounts of solubilized proteins were loaded on 4–20% gradient SDS-PAGE gels (Bio-Rad), blotted onto nitrocellulose membranes and incubated with the following primary antibodies: HSL (#4107), ATGL (#2138) and GAPDH (#2118) were purchased from CST Ozyme; total PDHE1 $\alpha$  (#Ab110334), phospho-Ser293 PDHE1 $\alpha$  (#Ab177461), UCP1 (#Ab10983) and GLUT1 (#Ab40084) from Abcam; PLIN5 (#GP31) and PLIN 1 (#GP29) from PROGEN; PDK4 (#H00005166-A02) from Abnova and PCK1 (#AP8093b) from Abgent. Anti-rabbit or anti-mouse IgG coupled to horseradish peroxidase were used as secondary antibodies. Immunoreactive proteins were determined by chemiluminescence (Clarity, Bio-Rad) with a ChemiDoc MP System (Bio-Rad) and quantification was performed using Image Lab software (Bio-Rad).

#### 2.1.5. Substrate oxidation

Oleic acid oxidation and incorporation into triglycerides were assessed as described in Ref. [41]. To determine pyruvate oxidation, insulin was removed from culture medium the day before assay. Cells were incubated for 3 h in 1 ml Krebs–Ringer Buffer (125 mM NaCl, 5 mM KCl, 2 mM CaCl $_2$ , 1.25 mM KH $_2$ PO $_4$ , 1.25 mM MgSO $_4$ , 25 mM NaHCO $_3$ ) supplemented with 2% BSA, 10 mM HEPES, 2 mM glucose, 1 mM pyruvate and 0.5  $\mu$ Ci [1- $^{14}$ C]-pyruvic acid (PerkinElmer) with or without 100 nM insulin. Medium was then acidified with 1 M sulfuric acid in closed vials containing a central well filled with benzethonium hydroxide. After 3 h incubation, trapped  $^{14}$ CO $_2$  was measured by liquid scintillation counting. Specific activity was measured and used to determine the quantity of oxidized pyruvate equivalent. Cells were washed with PBS and scraped in STED buffer (0.25 M sucrose, 10 mM Tris–HCl, 1 mM EDTA, 1 mM dithiothreitol, pH 7.4). Results were normalized to protein content determined with Bio-Rad protein assay using BSA as standard.

#### 2.1.6. Oxygen consumption

hMADS cells were seeded in 24 multi-well plates (Seahorse Bioscience) and differentiated as described above. Oxygen consumption rates (OCR) of 18 day-differentiated cells were determined using an XF24 Extracellular Flux Analyzer (Seahorse Bioscience). Basal OCR was calculated by subtraction of rotenone- and antimycin A-induced OCR (1  $\mu$ M of each inhibitor) to the unstimulated OCR value. Analyses were also carried out in

the presence of 50  $\mu\text{M}$  etomoxir, a carnitine palmitoyltransferase 1 (CPT1) inhibitor. Maximal respiration was determined using FCCP (1  $\mu\text{M}$ ). Oleate- and pyruvate-driven OCR were measured after addition of 200  $\mu\text{M}$  oleate and 5 mM pyruvate, respectively.

### 2.1.7. Lipolysis and re-esterification flux

Lipolysis was carried out as previously described [42]. Briefly, after an overnight loading period, lipolysis of [9,10- $^3\text{H}$ ]-oleic acid (PerkinElmer) was initiated by 1  $\mu\text{M}$  of  $\beta$ -adrenergic receptor agonist isoproterenol with or without 10  $\mu\text{M}$  triacsin C, an acyl-CoA synthetase inhibitor, to avoid fatty acid re-esterification. [9,10- $^3\text{H}$ ]-oleic acid and glycerol released in the medium were measured respectively by liquid scintillation counting and commercially available kit (Sigma). The results were normalized to total protein content of cell extracts.

Glyceroneogenesis was measured by the incorporation of [1- $^{14}\text{C}$ ]-pyruvic acid (PerkinElmer) into glycerol. Neutral lipids were extracted after pyruvic acid oxidation by adding 5 volumes chloroform:methanol (2:1) on cell lysate. After centrifugation, the organic phase was dried and hydrolyzed in 1 ml 0.25 N NaOH in chloroform:methanol (1:1) for 1 h at 37  $^{\circ}\text{C}$ . The solution was neutralized with 500  $\mu\text{l}$  0.5 N HCl in methanol. Fatty acids and glycerol were separated by adding 1.7 ml chloroform, 860  $\mu\text{l}$  water and 1 ml chloroform:methanol (2:1). Incorporation of  $^{14}\text{C}$ -carbon into glycerol was measured in the upper phase by liquid scintillation counting.

Glycerol kinase activity was assessed by the incorporation of [U- $^{14}\text{C}$ ]-glycerol (PerkinElmer) into triglycerides. Briefly, hMADS cells were incubated for 3 h in differentiation medium without glucose and pyruvate to avoid glyceroneogenesis. Then, fresh glucose/pyruvate-free differentiation medium supplemented with 0.3% BSA, 100  $\mu\text{M}$  glycerol and 1  $\mu\text{Ci}$  [U- $^{14}\text{C}$ ]-glycerol was added. After 2 h, the cells were washed with PBS and scraped with STED buffer for protein normalization. Neutral lipids were extracted and separated by thin layer chromatography to measure glycerol incorporation into triglycerides.

### 2.1.8. Pyruvate concentration

The day before the assay, insulin was removed from the culture medium. Cells were washed with PBS and incubated in glucose/pyruvate-free differentiation medium supplemented with 7.8 mM glucose. After 3 h, pyruvate released in the medium was measured using commercially available kit (BioAssay Systems). Cells were scraped in RIPA buffer for protein normalization.

### 2.1.9. Glucose uptake and *de novo* lipogenesis

Glucose uptake was measured using [1,2- $^3\text{H}$ ]-2-deoxy-D-glucose as previously described [43]. *De novo* lipogenesis was determined by [1- $^{14}\text{C}$ ]-acetic acid incorporation into triglycerides. The day before the assay, insulin was removed from the culture medium. Cells were incubated for 3 h in Krebs–Ringer buffer (*cf.* Section 2.1.5) supplemented with 2% BSA, 10 mM HEPES, 2 mM glucose, 5 mM acetate and 2  $\mu\text{Ci}$  [1- $^{14}\text{C}$ ]-acetic acid (PerkinElmer), in the presence or absence of 100 nM insulin. Cells were scraped in STED buffer and neutral lipids were separated by thin layer chromatography.

### 2.1.10. RNA interference

mRNA knockdown was achieved using small interfering RNA (siRNA). Briefly, on day 7 of differentiation, hMADS cells were detached from culture dishes with trypsin/EDTA (Invitrogen) and counted. One hundred picomol of a pool of either 4 siRNAs targeting PDK4 or 4 non-targeted control siRNAs (ThermoFischer Scientific) were delivered into adipocytes by a microporator (Invitrogen), with the following parameters: 1,100 V, 20 ms, 1 pulse. The targeted sequences were: siControl pool 1:

5'-UGGUUUACAUGUCGACUAA-3'; siControl pool 2: 5'-UGGUUUACAUGUUGUGUGA-3'; siControl pool 3: 5'-UGGUUUACAUGUUUCUGA-3'; siControl pool 4, 5'-UGGUUUACAUGUUUCCUA-3'; siPDK4 pool 1: 5'-GACCCGCUCUUAGUUUAUA-3'; siPDK4 pool 2: 5'-CAACGCCUGUGAUGGAUA-3'; siPDK4 pool 3: 5'-CGACAAGAAUUGCCUGUGA-3'; siPDK4 pool 4: 5'-GAGCAUUUCUCGCGCUACA-3'.

### 2.2. Human primary adipocytes

Human subcutaneous abdominal adipose tissue was collected from abdominoplasty of healthy patients for stromavascular fraction isolation according to the procedure previously described [29]. Stromavascular fraction cells were plated and maintained in DMEM containing 10% FCS until confluence. Differentiation of primary cultures was performed according to the protocol described for hMADS cells.

### 2.3. *In vivo* mouse studies

Mouse studies were performed in accordance with French and European animal care facility guidelines. A first cohort of 21 week-old PPAR $\alpha$ -null male mice on C57BL/6J genetic background and their wild-type (WT) counterparts were acclimated at thermoneutral temperature (30  $\pm$  1  $^{\circ}\text{C}$ ) for 4 weeks, on a 12/12 h light/dark cycle with *ad libitum* water and food. Mice were treated for 10 days with the  $\beta_3$ -adrenergic receptor agonist CL316,243 (0.1 mg/kg/d) (Sigma) or vehicle (DMSO) by daily intraperitoneal injections. A second cohort of 10 week-old mice was housed at standard room temperature (21  $\pm$  1  $^{\circ}\text{C}$ ). Mice were treated for 7 days with CL316,243 (1 mg/kg) or vehicle by daily intraperitoneal injections. After an overnight fast, mice were killed by cervical dislocation, and tissues were rapidly sampled and frozen in liquid nitrogen before being stored at  $-80^{\circ}\text{C}$ .

#### 2.3.1. mRNA expression

Inguinal WAT or interscapular BAT samples were homogenized in Qiazol buffer (Qiagen) using Precellys homogenizer (Ozyme). Total RNA samples were processed as described in Section 2.1.2. SYBR Green primers (Eurogentec) and Taqman probes (Life Technologies) are listed in Tables S1 and S2.

#### 2.3.2. Western blot

Tissues were powdered in liquid nitrogen and homogenized in RIPA buffer (Sigma) containing cocktail of protease and phosphatase inhibitors (Sigma). Western blotting was then performed as described in Section 2.1.4. Proteins of interest were normalized to total blotted proteins by using stain-free gels (Bio-Rad).

#### 2.4. Statistical analyses

Statistical analyses were performed using GraphPad Prism (GraphPad Software v.5.0). Paired or unpaired one-way ANOVA were performed and followed by Tukey's *post hoc* test to determine differences between groups. Two-way ANOVA, followed by Bonferroni's *post hoc* test, was applied when appropriate. Data are presented as percent of control cells or percent of WT untreated-mice,  $\pm$ SEM, unless otherwise described in legend. Statistical significance was set at  $p < 0.05$ .

## 3. RESULTS

### 3.1. PPAR $\gamma$ and PPAR $\alpha$ agonists promote browning of human white adipocytes

Treatments with PPAR $\gamma$  (Rosi) or PPAR $\alpha$  (GW) agonists added for 4 days on differentiated white adipocytes (Figure S1A) increased UCP1 mRNA and protein levels (15- and 11-fold increase, respectively) (Figure 1A,B), as well as expression of genes classically elevated in

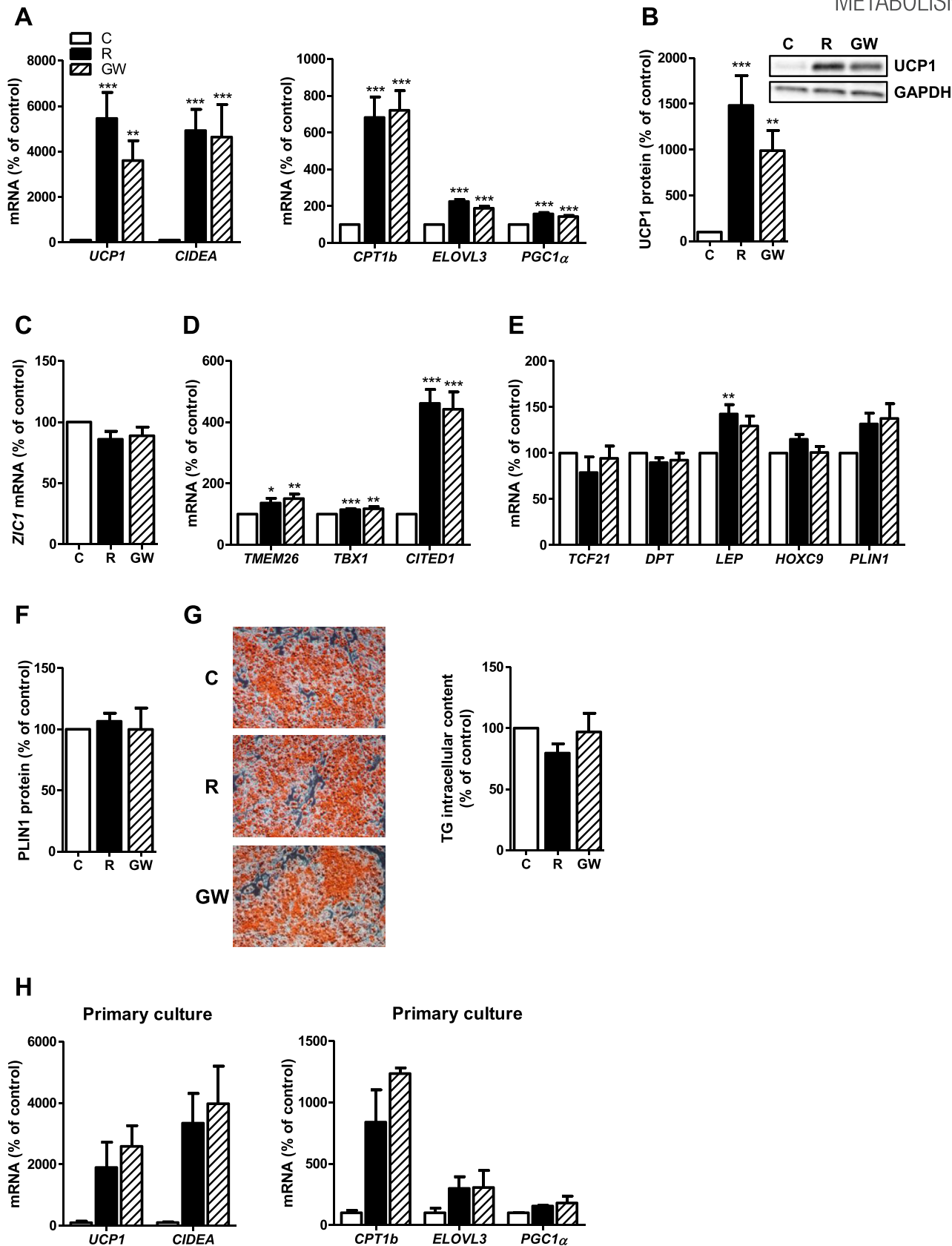


**Figure 1: PPAR $\gamma$  and PPAR $\alpha$  agonists promote browning of human white adipocytes.** (A) Gene expression levels of thermogenic genes. (B) UCP1 protein content. Gene expression levels of (C) brown-, (D) brite- and (E) white-specific markers. (F) PLIN1 protein content. (G) Pictures representative of Oil Red O staining in each condition at day 18. Intracellular triglyceride (TG) content quantified by enzymatic assay. (H) mRNA levels of thermogenic genes in human adipocytes differentiated in primary culture. Data represent mean  $\pm$  SEM expressed as percentage of control ( $n = 6-12$ ) for hMADS cells and ( $n = 2-4$ ) for primary adipocytes. Open bars: control cells (C), full bars: rosiglitazone-treated cells (R), hatched bars: GW7647-treated cells (GW). \*:  $p < 0.05$  for R or GW vs. C; \*\*:  $p < 0.01$ ; \*\*\*:  $p < 0.001$ .

**Table 1** — Significantly enriched biological processes among genes upregulated by rosiglitazone and GW7647.

Biological processes	Upregulated by rosiglitazone	Upregulated by GW7647
	p Value	p Value
GO:0006631_Fatty acid metabolic process	6.76E-08	2.16E-11
GO:0006635_Fatty acid beta-oxidation	6.76E-05	1.96E-11
GO:0008610_Lipid biosynthetic process	7.55E-05	8.26E-06
GO:0009062_Fatty acid catabolic process	2.16E-04	7.59E-10
GO:0019395_Fatty acid oxidation	3.08E-04	2.00E-09
GO:0034440_Lipid oxidation	3.08E-04	2.00E-09
GO:0019216_Regulation of lipid metabolic process	9.86E-04	6.76E-04
GO:0030258_Lipid modification	1.14E-03	3.38E-07
GO:0044242_Cellular lipid catabolic process	2.07E-03	1.51E-07
GO:0016042_Lipid catabolic process	2.49E-02	2.66E-04
GO:0051181_Cofactor transport	2.51E-02	1.37E-02
GO:0006767_Water-soluble vitamin metabolic process	3.07E-02	3.16E-02
GO:0050873_Brown fat cell differentiation	3.63E-02	2.24E-02
GO:0005996_Monosaccharide metabolic process	3.78E-02	5.76E-03
GO:0019318_Hexose metabolic process	3.83E-02	3.75E-03
GO:0010876_Lipid localization	3.97E-02	3.38E-02
GO:0019217_Regulation of fatty acid metabolic process	4.87E-02	1.80E-02

p Values are adjusted by Benjamini correction.

brown and brite fat cells (*CIDEA*, *CPT1b*, *ELOVL3*, *PGC1 $\alpha$* ) (Figure 1A). We next determined whether PPAR agonist-treated adipocytes expressed brown- and brite-specific markers. Brown markers were not (*MPZL* and *LHX8*) expressed or were weakly (*ZIC1*) expressed and not regulated by treatments (Figure 1C and data not shown). By contrast, expression of brite adipocyte markers *TMEM26*, *TBX1* and *CITED1* was increased (Figure 1D). Altogether, these data indicate that upon PPAR $\gamma$  or PPAR $\alpha$  activation, hMADS white adipocytes display a molecular pattern of brite fat cells.

Gene expression levels of the white adipocyte markers *TCF21*, *DPT*, *LEP*, *HOXC9* and *PLIN1* were barely, or not at all, regulated by PPAR agonists (Figure 1E). Accordingly, protein level of *PLIN1* was not modified by treatments (Figure 1F). Triglyceride content of differentiated adipocytes was not altered (Figure 1G). The two PPAR agonists induced down-regulation of PPAR $\gamma$  mRNA level with no effect on other members of the PPAR family (Figure S1B).

The results were confirmed in primary human differentiated pre-adipocytes. In Rosi- and GW-treated primary adipocytes, mRNA expression of *UCP1* and of several other thermogenic genes was upregulated (Figure 1H), while white and adipogenic markers were not changed (Figure S1C). mRNA levels of the brite markers *TBX1* and *CITED1* increased as observed in treated hMADS cells (Figure S1D).

### 3.2. PPAR $\gamma$ and PPAR $\alpha$ agonists drive similar transcriptional response and mitochondrial adaptation in white adipocytes

DNA microarrays were used to investigate the whole transcriptional effects of PPAR $\gamma$  and PPAR $\alpha$  agonists on hMADS cells. SAM analysis of 12891 transcripts using false discovery rate of 5% revealed that, compared to untreated white adipocytes, 265 and 210 genes were significantly up- and down-regulated by Rosi, respectively, and 470 and 209 genes were significantly up- and down-regulated by GW, respectively (data not shown).

Among the 215 genes upregulated by the two treatments, 96 and 57 were induced by more than 3-fold by Rosi and GW, respectively. On the contrary, genes upregulated specifically by Rosi or GW displayed weak fold induction, suggesting major overlap in the regulation of gene expression by PPAR $\gamma$  and PPAR $\alpha$  agonists in adipocytes. Consistent with these findings, several lipid metabolism-related biological processes were found to be regulated by both Rosi and GW (Table 1). RT-qPCR confirmed that expression of genes involved in fatty acid uptake, activation and esterification was increased in brite fat cells (Figure S2A). Gene ontology analysis also revealed that both fatty acid anabolism and catabolism were activated during briteening (Table 1 and Table S3) as confirmed by RT-qPCR data of major genes driving triglyceride synthesis and fatty acid oxidation (Figure 1A and Figure S2B,C). A few genes showed down-regulated expression. Fold changes were markedly lower than upregulated genes: only 14 out of 210 and 4 out of 209 genes were decreased by more than 3-fold by Rosi and GW, respectively.

Collectively, these results show that the two agonists have a profound effect on fatty acid anabolic and catabolic pathways.

Besides fatty acid metabolism, DNA microarrays showed upregulation of a number of mitochondrial genes by Rosi and GW. RT-qPCR measurements confirmed the upregulation of several subunits of the mitochondrial electron transport chain (Figure S2D). This was associated with slightly higher mitochondrial biogenesis assessed by mitochondrial DNA content (Figure S2E) and a sharp increase in maximal oxygen consumption in brite adipocytes (Figure S2F). Given the weak induction of mitochondrial biogenesis compared to the boosted mitochondrial respiration, our results suggest major metabolic adaptations associated with briteening.

### 3.3. Briteening of white adipocytes induces anabolic and catabolic pathways of fat metabolism

Briteening of hMADS adipocytes was associated with increased oleate incorporation into triglycerides as suggested by gene upregulation (Figure 2A, Figure S2A and Table S3). Newly activated fatty acids require glycerol-3-phosphate as a backbone for esterification. Glycerol kinase, an enzyme with higher expression in BAT than in WAT, showed strong induction in response to the treatments (Figure 2B). Accordingly, glycerol incorporation into triglycerides was enhanced (Figure 2C).

Increased fat synthesis was associated with enhanced triglyceride breakdown. The lipolytic capacity assessed by glycerol release into the medium in response to isoproterenol, a pan  $\beta$ -adrenergic receptor agonist, was enhanced (Figure 2D), along with increase of mRNA and protein expression of the two main lipases: ATGL and HSL (Figure 2E and Figure S3A). Gene expression of AQP7, a transporter facilitating glycerol efflux, was also upregulated (Figure S3B).

In line with the induction of numerous genes involved in fatty acid mitochondrial transport and oxidation (Table S3), briteening sharply increased oleate oxidation (Figure 2F). mRNA and protein levels of *PLIN5*, a lipid droplet binding protein involved in fatty acid oxidation, were strongly enhanced (Figure 2G and Figure S2C). Oxygen consumption in brite adipocytes was higher than in white fat cells (Figure 2H). After addition of etomoxir, a carnitine palmitoyltransferase 1 inhibitor, the oxygen consumption of brite adipocytes was blunted to the level of white adipocytes (Figure 2H), indicating that, in contrast to white fat cells, the higher metabolic rate of brite fat cells is linked to fatty acid oxidation. In agreement with these results, oleate addition increased OCR only in brite adipocytes (Figure 2I), further demonstrating the elevated capacity of brite fat cells to oxidize fatty acids.

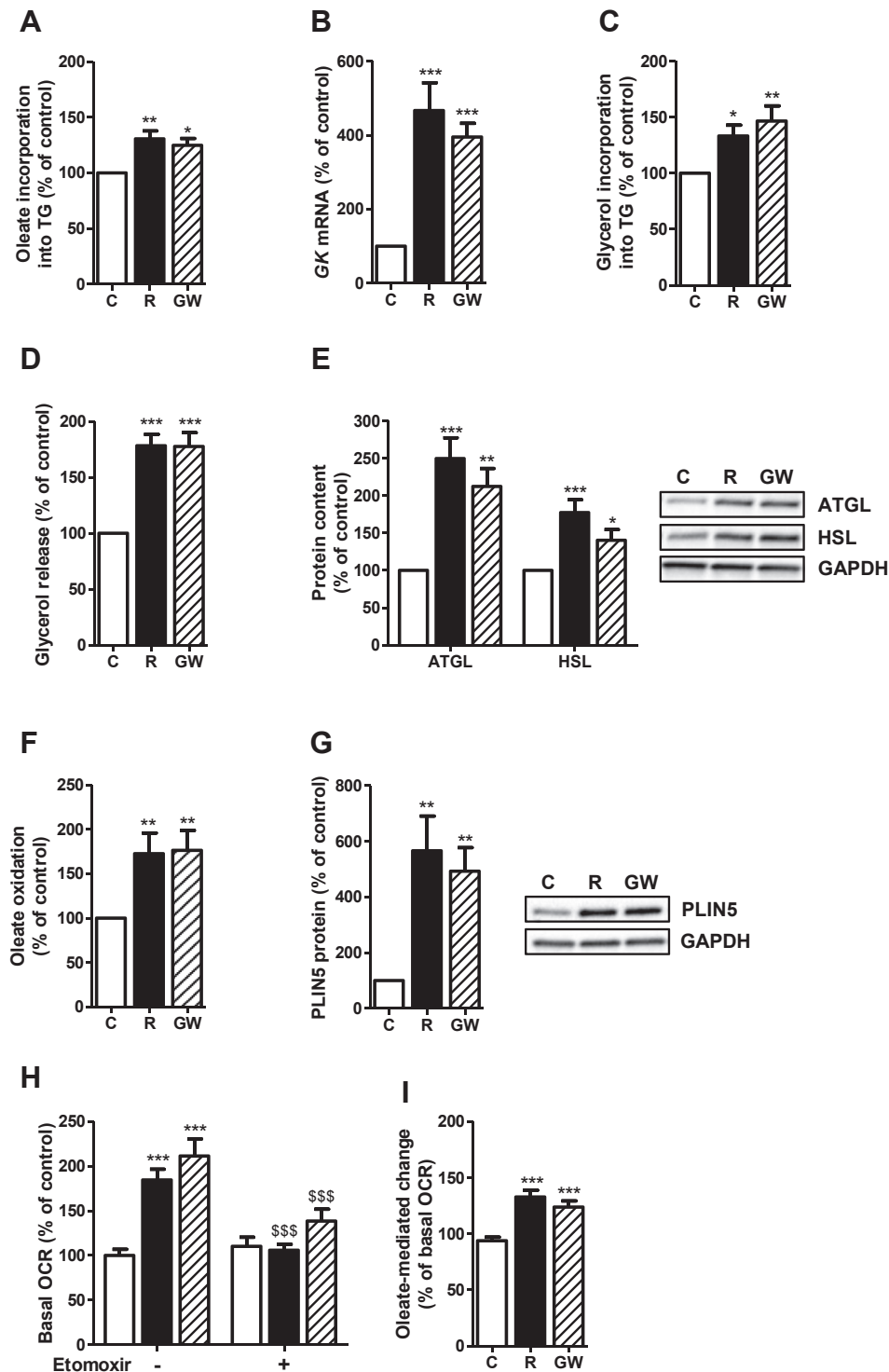


**Figure 2: Britening of white adipocytes induces anabolic and catabolic pathways of fat metabolism.** Fatty acid metabolism was investigated in 18 day-differentiated hMADS cells treated or not with rosiglitazone or GW7647 for the last 4 days. (A) Fatty acid (oleate) incorporation into triglycerides (TG). (B) Gene expression level of glycerol kinase (*GK*). (C) Glycerol incorporation into triglycerides. (D) Glycerol release after stimulation by the  $\beta$ -adrenergic agonist, isoproterenol. (E) ATGL and HSL protein content. (F) Fatty acid (oleate) oxidation. (G) PLIN5 protein content. (H) Basal mitochondrial oxygen consumption rates (OCR) in the presence or not of 50  $\mu$ M etomoxir. (I) OCR measured after addition of 200  $\mu$ M oleate. Data represent mean  $\pm$  SEM expressed as percentage of control ( $n = 7-12$ ). Open bars: control cells (C), full bars: rosiglitazone-treated cells (R), hatched bars: GW7647-treated cells (GW). \*:  $p < 0.05$  for R or GW vs. C; \*\*:  $p < 0.01$ ; \*\*\*:  $p < 0.001$ . \$\$\$:  $p < 0.001$  for etomoxir vs. basal condition.

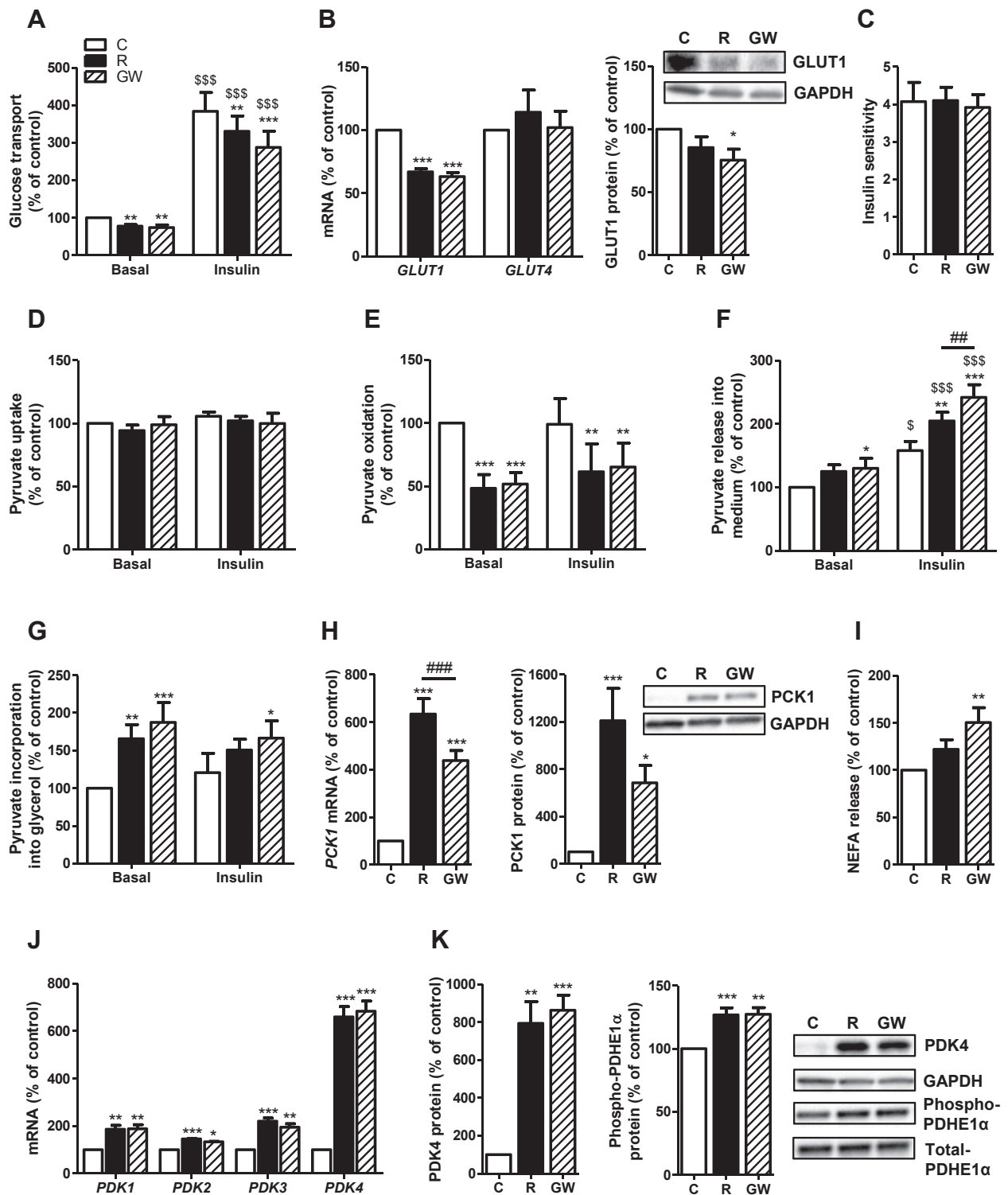


**Figure 3: Britening of white adipocytes promotes a shift of glucose metabolism from oxidation towards glycerol production.** Glucose metabolism was investigated in 18 day-differentiated hMADS cells treated or not with rosiglitazone or GW7647 for the last 4 days. (A) Glucose transport in the presence or not of 100 nM insulin. (B) Gene expression levels of the glucose transporters *GLUT1* and *GLUT4* and GLUT1 protein level. (C) Insulin sensitivity estimated by the insulin stimulated-to-basal glucose uptake ratio. (D) Pyruvate uptake, (E) pyruvate oxidation and (F) pyruvate release into the medium in the presence or not of 100 nM insulin. (G) Glyceroneogenesis assessed by incorporation of pyruvic acid into the glycerol moiety of neutral lipids. (H) PCK1 mRNA and protein levels. (I) Lipolysis measured by oleic acid release into the medium after stimulation by the  $\beta$ -adrenergic agonist, isoproterenol. (J) Gene expression levels of the four *PDK* isoforms. (K) PDK4 and Ser293-phosphorylated PDHE1 $\alpha$  protein levels. Data represent mean  $\pm$  SEM expressed as percentage of control (n = 6–12). Open bars: control cells (C), full bars: rosiglitazone-treated cells (R), hatched bars: GW7647-treated cells (GW). \*: p < 0.05 for R or GW vs. C; \*\*: p < 0.01; \*\*\*: p < 0.001. \$: p < 0.05 for insulin vs. unstimulated condition; \$\$\$: p < 0.001. ##: p < 0.01 for R vs. GW; ###: p < 0.001.

Taken together, these data show that briteing of white adipocytes is associated with major adaptations in fatty acid metabolism, promoting both triglyceride synthesis and hydrolysis and driving fatty acid fluxes towards mitochondrial oxidation.

### 3.4. Briteing of white adipocytes promotes a shift of glucose metabolism from oxidation towards glycerol production

Basal and insulin-stimulated glucose uptakes were decreased in brite adipocytes (Figure 3A). This was consistent with decreased mRNA and protein levels of the glucose transporter GLUT1 (Figure 3B). *GLUT1* expression was strongly correlated with basal glucose transport (Figure S4A). Insulin sensitivity evaluated by the insulin stimulated-to-basal glucose uptake ratio was preserved (Figure 3C) as was gene expression level of the insulin-responsive glucose transporter *GLUT4* (Figure 3B).

To directly assess glucose oxidation without the confounding effect of changes in glucose uptake and glycolysis, we used radiolabelled pyruvate, the end-product of glycolysis. Pyruvate uptake was not modified by the treatments (Figure 3D). Briteing decreased pyruvate oxidation by up to 50% in basal and insulin-stimulated conditions (Figure 3E). Pyruvate flux was redirected towards other pathways in brite adipocytes as shown by higher pyruvate release into the medium (Figure 3F) and by activation of glyceroneogenesis leading to increased incorporation of pyruvate into the glycerol backbone of neutral lipids (Figure 3G). This glycerol-3-phosphate synthesis pathway is highly dependent on phosphoenolpyruvate carboxykinase 1 (PCK1) activity, which mRNA and protein levels were sharply increased in response to Rosi and GW (Figure 3H). Glycerol-3-phosphate dehydrogenase 1 gene expression was also upregulated in brite adipocytes (Figure S4B). The newly formed glycerol-3-phosphate allowed fatty acid re-esterification, which is demonstrated by the moderate release of fatty acids compared to glycerol following  $\beta$ -adrenergic receptor agonist stimulation (Figures 2D and 3I). To directly assess glucose carbon incorporation into fatty acids *i.e.*, *de novo* lipogenesis, radiolabelled acetate was used. The change in brite adipocytes was marginal as was the changes in cognate gene expression (Figure S4C,D).

These results point at intracellular pyruvate as a central node in brite adipocyte glucose metabolism. One of the top-ranking genes upregulated by the two treatments in the DNA microarray analyses and confirmed by RT-qPCR (Figure 3J) was pyruvate dehydrogenase kinase 4 (*PDK4*), which phosphorylates the pyruvate dehydrogenase complex (PDH). *PDK4* protein level was strongly upregulated, leading to higher PDH phosphorylation on the E1 $\alpha$  subunit in brite adipocytes (Figure 3K). *PDK1*, 2 and 3 were more modestly upregulated during briteing (Figure 3J). In human primary adipocytes, PPAR agonists also upregulated *PDK4* gene expression (Figure S4E).

Altogether, our observations show that, in human brite adipocytes, glucose metabolism switches from oxidation towards glycerol-3-phosphate production, favoring triglyceride synthesis. Moreover, the strong induction of *PDK4*, through phosphorylation of the PDH complex, invokes a shift in fuel selection favoring oxidation of fatty acids instead of glucose.

### 3.5. PDK4 knockdown prevents induction of fatty acid oxidation in brite adipocytes

To directly address the role of *PDK4* in the metabolic remodeling associated with briteing of hMADS cells, siRNA-mediated knockdown was validated at mRNA and protein levels (Figure 4A). There was no alteration in the expression of *UCP1*, brown and brite markers and of other *PDK* isoforms (Figure 4B and Figure S5A,B). Decreased *PDK4* expression resulted in lower PDH phosphorylation (Figure 4C).

Consequently, pyruvate release from brite adipocytes was decreased to the levels observed in white adipocytes (Figure 4D) and briteing-induced glyceroneogenesis was partially inhibited (Figure 4E). Concomitantly, *PDK4* knockdown restored pyruvate oxidation in brite fat cells (Figure 4F). Consistent with higher pyruvate oxidation, pyruvate-driven OCR raised by up to 50% over basal in white and *PDK4* siRNA-treated brite adipocytes while brite adipocytes did not respond to pyruvate addition (Figure S5C). Contrary to pyruvate oxidation, *PDK4* siRNA treatment blunted fatty oxidation in brite adipocytes (Figure 4G). Basal OCR in brite adipocytes, which is highly dependent on fatty acid oxidation (Figure 2H,I), returned to white fat cell level upon *PDK4* knockdown (Figure S5D), similarly to what was observed when fatty acid oxidation was prevented by etomoxir (Figure 2H). However, fatty acid oxidation remained higher in *PDK4* siRNA-treated brite compared to white adipocytes (Figure 4G), suggesting that other mechanisms such as increased expression of fatty acid metabolism genes (Figure S5A and Table S3) were involved. Fatty acid esterification was not altered by *PDK4* knockdown (Figure S5E), demonstrating that *PDK4* specifically regulates the oxidative metabolism of fatty acids. Collectively, these results suggest that *PDK4* has a major role, independently of the briteing process *per se*, in regulating the preference for fatty acids over glucose for mitochondrial oxidation of brite fat cells.

### 3.6. PPAR $\alpha$ deficiency disrupts WAT briteing-induced *PDK4* expression *in vivo*

Data in human adipocytes indicated that *PDK4* induction was responsible for major metabolic adaptations during briteing. To confirm these *in vitro* results, we aimed at investigating *PDK4* regulation *in vivo*. As PPAR $\gamma$  but not PPAR $\alpha$  deficiency in WAT provokes lipodystrophy, PPAR $\alpha$ -null mice were used. Inguinal WAT was investigated as it is a fat depot prone to briteing compared to other fat pads.

Two cohorts of mice were investigated. WT and PPAR $\alpha$ -null mice at 21 weeks of age acclimated at thermoneutrality were treated with the  $\beta_3$ -adrenergic agonist CL316,243. Acclimation to thermoneutrality is essential to avoid the confounding effects due to activation of brown and brite fat depots at conventional housing temperature. Body weight and inguinal fat pad weight were higher in PPAR $\alpha$ -null mice compared to age-matched WT mice (Figure S6A). As the difference in adiposity between genotypes may influence briteing in inguinal fat pad and obesity in PPAR $\alpha$ -null mice develops with aging [44], CL treatment was applied to younger mice housed at standard temperature. As expected, there was no difference in body and inguinal fat pad weights between 11 week-old WT and PPAR $\alpha$ -null mice (Figure S6B). *Ppar $\alpha$*  mRNA was, respectively, undetectable and expressed at low level in inguinal WAT of vehicle-treated PPAR $\alpha$ -null and WT mice and was induced upon chronic  $\beta_3$ -adrenergic stimulation only in WT mice (Figure S6C,D). *UCP1* mRNA and protein were barely detectable in WAT of vehicle-treated WT and PPAR $\alpha$ -null mice. Upon CL316,243 treatment, *UCP1* expression in WAT was sharply induced in WT mice while this increase was markedly blunted in PPAR $\alpha$ -null mice (Figure 5A,B). PPAR $\alpha$  deficiency did not impair white adipogenesis as shown by similar expression of *Ppar $\gamma$*  and *Dpt*, a white adipocyte specific marker [35], in both WT and PPAR $\alpha$ -null mice (Figure S6E). Inguinal WAT mRNA levels of the classical markers of thermogenic cells, *Cidea* and *Cpt1b*, were barely detectable in vehicle-treated mice and sharply increased upon  $\beta_3$ -adrenergic agonist treatment in WT mice, while this induction was impaired in PPAR $\alpha$ -null mice as thermogenic genes (Figure 5C,D). Classical brite adipocyte markers such as *Cited1* and *Tmem26* displayed the same pattern (Figure 5E,F). Noteworthy, the expression of these genes was induced by CL316,243 in interscapular BAT of both WT and PPAR $\alpha$ -null mice (Figure S6F), suggesting a

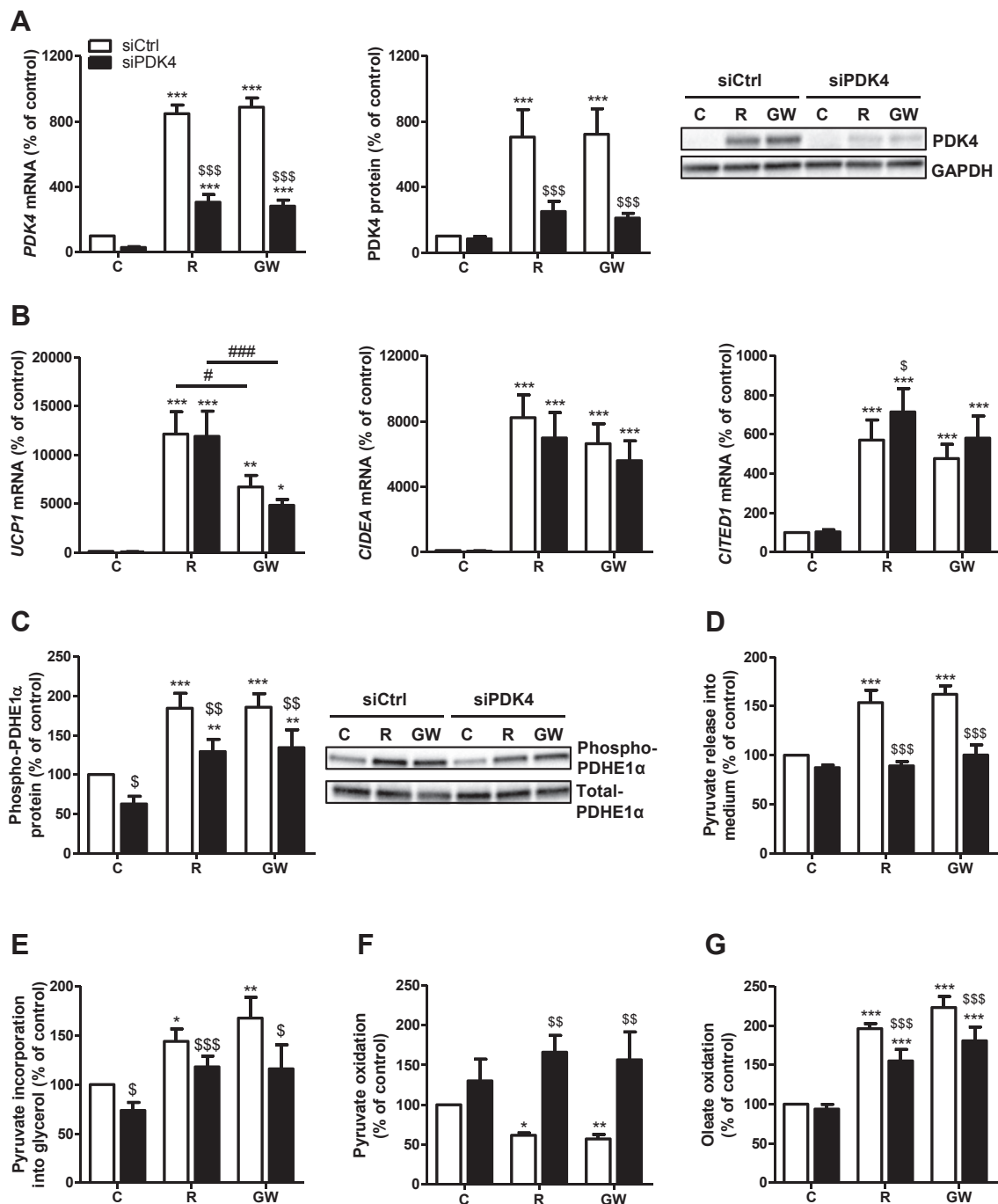


**Figure 4: PDK4 knockdown prevents induction of fatty acid oxidation in brite adipocytes.** Britening-associated changes were explored in 18 day-differentiated hMADS cells transfected with either a control-or PDK4-targeting siRNA and treated or not with rosiglitazone or GW7647 for the last 4 days. (A) PDK4 mRNA and protein levels. (B) Gene expression levels of *UCP1*, *CIDEA* and *CITED1*. (C) Ser293-phosphorylated PDHE1 $\alpha$  protein levels. (D) Pyruvate release into the medium. (E) Glycero-neogenesis assessed by incorporation of pyruvic acid into the glycerol moiety of neutral lipids. (F) Pyruvate oxidation. (G) Fatty acid (oleate) oxidation. Data represent mean  $\pm$  SEM expressed as percentage of control (n = 6–11). Open bars: siCtrl-treated cells, full bars: siPDK4-treated cells. \*: p < 0.05 for R or GW vs. C; \*\*: p < 0.01; \*\*\*: p < 0.001. \$: p < 0.05 for siPDK4 vs. siCtrl; \$\$: p < 0.01; \$\$\$: p < 0.001. #: p < 0.05 for R vs. GW; ###: p < 0.001.

specific role of PPAR $\alpha$  in brite fat cells compared to brown fat cells upon chronic  $\beta_3$ -adrenergic stimulation. PDK4 expression was up-regulated in inguinal WAT at mRNA and protein levels during CL316,243 treatment in WT mice, while this induction was severely blunted in PPAR $\alpha$ -null mice (Figure 5G,H). Supporting the induction of PDK4 as a

major feature of britening, PDK4 expression was strongly correlated with UCP1 expression at both protein and mRNA levels in inguinal WAT (Figure 5I and Figure S6G).

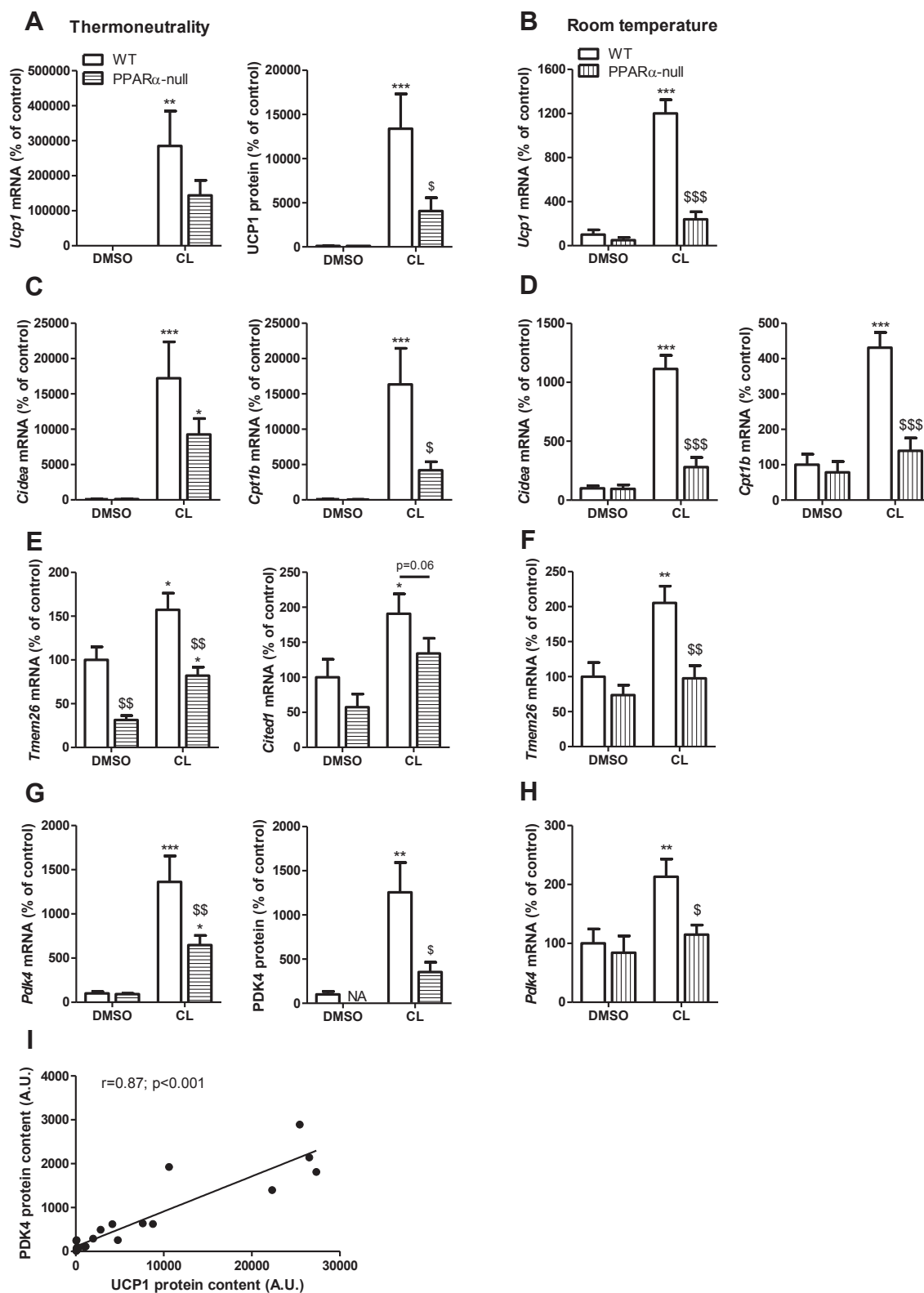


**Figure 5: PPAR $\alpha$  deficiency disrupts WAT browning-induced PDK4 expression *in vivo*.** (A, C, E, G and I) WT and PPAR $\alpha$ -null male mice housed at thermoneutrality were treated with CL316,243 (CL, 0.1 mg/kg/d) or vehicle (DMSO) for 10 days. (B, D, F and H) WT and PPAR $\alpha$ -null male mice housed at standard temperature were treated with CL316,243 (CL, 1 mg/kg/d) or vehicle (DMSO) for 7 days. Analyses were performed on the inguinal white adipose tissue depot. (A, B) UCP1 mRNA and protein levels. (C–F) Gene expression levels of *Cidea*, *Cpt1b*, *Cited1* and *Tmem26*. (G, H) PDK4 mRNA and protein levels. (I) Spearman correlation between UCP1 and PDK4 protein content (n = 23). Data represent mean  $\pm$  SEM expressed as percentage of vehicle-treated WT mice (n = 7–9 mice per group). Open bars: wild-type mice, hatched bars: PPAR $\alpha$ -null mice. NA: not available. \*: p < 0.05 for CL vs. DMSO; \*\*: p < 0.01; \*\*\*: p < 0.001. \$: p < 0.05 for PPAR $\alpha$ -null vs. wild type; \$\$: p < 0.01; \$\$\$: p < 0.001.

#### 4. DISCUSSION

Understanding the role of brown and brite adipocytes in humans may result in strategies aimed at dissipating the energy surplus and improving metabolism in obesity and related disorders. Little is known about the metabolic adaptations during white-to-brite adipocyte conversion. Herein, we investigated the molecular and metabolic changes following chronic PPAR $\gamma$  or PPAR $\alpha$  activation of human mature white adipocytes. Our results robustly show that PPAR agonists are able to promote white-to-brite conversion as shown by a sharp induction of UCP1 as well as numerous thermogenic genes and brite adipocyte markers. DNA microarray experiments reveal that these agonists drive profound changes in energy metabolism. Britening promotes higher mitochondrial oxygen consumption which is associated with enhanced fatty acid anabolism and catabolism whereas glucose oxidation is diminished. Instead, glucose utilization is redirected towards glyceroneogenesis and favors triglyceride synthesis. The shift from glucose to fatty acid as preferential energy substrate is partly mediated by the metabolic switch PDK4. *In vivo*, PPAR $\alpha$ -null mice display altered UCP1 and PDK4 induction in inguinal WAT in response to  $\beta_3$ -adrenergic agonist-induced britening.

The brown identity of a fat cell relies on its capacity to sustain thermogenesis *i.e.*, to possess high mitochondrial oxidative capacities associated with activation of the *bona fide* uncoupling protein, UCP1. Here, we report that human mature white adipocytes can acquire these brown fat cell properties upon PPAR $\gamma$  or PPAR $\alpha$  activation. In addition to the upregulation of genes that characterize both brown and brite adipocytes compared to white fat cells, other markers have been identified in mouse studies to distinguish the brite from the brown cell type. Defining the molecular signature of human UCP1-positive adipocytes using murine brite-specific genes led to conflicting results reporting either classical brown [45–47] or brite [19,27,48] profiles, which may depend on the depth in the adipose depot considered [49]. These data were inferred from gene expression measurements in fat biopsies or in precursor cells differentiated *in vitro* in either white or brown/brite adipocytes. The profile of human mature white adipocytes converted into brown/brite cells has not been explored so far although this mechanism contributes *in vivo* to a great extent to the appearance of brite adipocytes in the mouse inguinal WAT depot [20,21]. Here, we provide evidence that human mature white adipocytes are capable of switching towards a brite phenotype since higher expression of brite markers is observed while classical brown genes are not regulated or poorly expressed.

PPAR $\gamma$  and PPAR $\alpha$  have well established roles in driving adipogenesis/triglyceride storage and fatty acid oxidation, respectively, in fat cells [50]. PPAR $\gamma$  role in brown fat cell differentiation has been extensively studied. The contribution of PPAR $\alpha$ , besides the regulation of fat utilization genes, is more elusive. Our data suggest that, in human white fat cells, PPAR $\gamma$  and PPAR $\alpha$  agonists have the same britening efficiency, as demonstrated by the wide overlap of regulated genes and by the absence of noticeable difference between the two treatments in any of the parameters investigated. The requirement of PPAR $\alpha$  for WAT britening is confirmed in PPAR $\alpha$ -null mice which display a disrupted induction of thermogenic and brite markers in the inguinal fat depot upon  $\beta_3$ -adrenergic agonist treatment. Our results support the findings that direct [32,33] or indirect [51,52] PPAR $\alpha$  activation in murine WAT and cultured white adipocytes promotes britening. Contrasting with WAT, we show that BAT response to CL316,243 treatment is similar in WT and PPAR $\alpha$ -null mice, which stresses that PPAR $\alpha$  is dispensable for activation of BAT as previously suggested [53]. These mechanistic differences between WAT britening and BAT activation further highlight

the need for suitable human cell models of white-to-brite conversion such as hMADS cells [54].

Classical detection of BAT activity *in vivo* relies on its capacity to take up high amounts of glucose in response to sympathetic stimulation. Unexpectedly, our data report a slight but significant lower basal glucose uptake in human brite adipocytes associated with a down-regulation of GLUT1 mRNA and protein levels. GLUT1 expression and basal glucose transport are highly correlated, further supporting the importance of GLUT1 in basal glucose uptake of hMADS adipocytes. In response to insulin, the magnitude of glucose uptake increase is the same in white and brite adipocytes, showing that insulin sensitivity is preserved. Differentiation of WAT precursor cells into brown-like fat cells has been associated with increased or decreased basal glucose uptake and GLUT1 expression, suggesting that browning and glucose uptake are not necessarily linked [55,56].

Britening of human white adipocytes is associated with an inhibition of carbohydrate oxidation and an upregulation of PDK4. These findings are consistent with the recent report by Loft et al. revealing that knockdown of the transcription factor KLF11 in hMADS adipocytes simultaneously impairs PPAR $\gamma$ -mediated browning and PDK4 upregulation [30]. Our *in vivo* data show that britening of WAT triggers sharp PDK4 mRNA and protein upregulation. Conversely, impaired britening in CL316,243-treated PPAR $\alpha$ -null mice is associated with lower PDK4 induction. PDK4 activity inhibits glucose-derived substrate oxidation through phosphorylation-mediated inactivation of the PDH complex. Consequently, PDH activity is blunted [57], making glucose available for energy substrate replenishment rather than for oxidation [58,59]. Pyruvate is redirected towards glyceroneogenesis to provide glycerol-3-phosphate backbone for fatty acid esterification [60]. Accordingly, glyceroneogenesis, the main glycerol-producing pathway in adipocytes [61], and its essential enzyme PCK1 are strongly induced during britening of human adipocytes. Concurrently, other glycerol-3-phosphate-producing pathways are activated *i.e.*, glycerol-3-phosphate dehydrogenase and glycerol kinase pathways. Interestingly, while PPAR $\alpha$  in liver controls glycerol uptake and conversion into glucose [62], our results show that britening of white adipocytes is associated with activation of glucose-derived glycerol production and release. This suggests a PPAR $\alpha$ -controlled *in vivo* metabolic crosstalk between adipose tissue and liver. PPAR $\alpha$  may control the britening of white adipocytes leading to enhanced glycerol release, which in turn can be used by the liver as a neoglucogenic substrate, another PPAR $\alpha$ -activated pathway. Additionally, we find that fatty acid esterification, lipolysis and fatty acid oxidation are simultaneously enhanced after britening both at the molecular and functional levels. The stimulation of both fatty acid esterification and degradation activates a futile triglyceride/fatty acid cycle contributing to intracellular fatty acid use and leading to a fine tuning of metabolic fluxes [61,63,64]. This mechanism may prevent an excessive release of fatty acids from fat depots known to promote lipotoxicity and insulin resistance. Importantly, these combined metabolic adaptations occur in the absence of changes in triglyceride content, and thus may not aggravate obesity at the whole-organism level.

As glucose is spared to supply replenishing pathways with britening, fatty acids become the favorite substrate for mitochondrial oxidation. This is demonstrated by higher fatty acid oxidation in brite adipocytes, whose induction is inhibited when glucose availability for oxidation is restored after PDK4 knockdown. It is noteworthy that the higher basal oxygen consumption in brite adipocytes returns to control value when fatty acid oxidation is prevented by etomoxir, further supporting the affinity of brite cells for fatty acids as mitochondrial substrates. These results are in agreement with *in vivo* findings showing that mice

treated with a  $\beta_3$ -adrenergic agonist exhibit higher whole-body fatty acid oxidation and lower respiratory quotient, indicative of a metabolic switch towards fat oxidation [65]. Furthermore, mice treated with niacin in order to block lipolysis show an altered thermogenic response, suggesting that fatty acids are the main energy source for thermogenesis in activated rodent BAT [59]. Consistent with mice data, clinical studies report a rapid decrease of BAT triglyceride content in cold-exposed patients, further pointing to fatty acids as the major energy substrates supplying thermogenic cells [66,67]. As it seems that cold-induced fatty acid oxidative metabolism in BAT is not impaired in type 2 diabetic patients [68], increasing the thermogenic capacity by white-to-brite adipocyte conversion appears as a valuable strategy.

## 5. CONCLUSION

Collectively, our results demonstrate for the first time that human mature white adipocytes can be converted into brite cells expressing thermogenic markers and displaying a wide metabolic reprogramming. We identified PDK4 as a crucial mediator redirecting glucose towards triglyceride synthesis, thereby favoring fatty acid use as energy substrate for uncoupling mitochondria. Human brite adipocytes are endowed with higher capacity for intra-adipose fatty acid oxidation and thus could be targeted to diminish fatty acid plasma level and their storage into ectopic insulin-sensitive tissues, in order to prevent obesity-associated insulin resistance and type 2 diabetes.

## ACKNOWLEDGMENTS

We gratefully acknowledge Frédéric Martins and Jean-José Maoret (Get-TQ transcriptomics facility) from the Institute of Metabolic and Cardiovascular Diseases (I2MC, Toulouse). We also thank Arnaud Polizzi (UMR1331 ToxAlim, Toulouse) for excellent technical assistance and Colette Bétoulières (UMR1331 ToxAlim, Toulouse) for mouse breeding and care. The authors also acknowledge the Cytomed Platform from IRCAN (Nice).

D.L. is a member of Institut Universitaire de France.

This work was supported by Inserm, CNRS, EU FP7 project DIABAT (HEALTH-F2-2011-278373), French Agence Nationale de la Recherche (ANR-10-BLAN-1105 miRBAT and ANR-12-BSV1-0025Obelip) and Région Midi-Pyrénées.

## CONFLICT OF INTEREST

None declared.

## APPENDIX A. SUPPLEMENTARY DATA

Supplementary data related to this article can be found at <http://dx.doi.org/10.1016/j.molmet.2016.03.002>.

## REFERENCES

- [1] Cannon, B., Nedergaard, J., 2004. Brown adipose tissue: function and physiological significance. *Physiological Reviews* 84:277–359.
- [2] Feldmann, H.M., Golozoubova, V., Cannon, B., Nedergaard, J., 2009. UCP1 ablation induces obesity and abolishes diet-induced thermogenesis in mice exempt from thermal stress by living at thermoneutrality. *Cell Metabolism* 9: 203–209.
- [3] Cypess, A.M., Lehman, S., Williams, G., Tal, I., Rodman, D., Goldfine, A.B., et al., 2009. Identification and importance of brown adipose tissue in adult humans. *The New England Journal of Medicine* 360:1509–1517.
- [4] van Marken Lichtenbelt, W.D., Vanhommerig, J.W., Smulders, N.M., Drossaerts, J.M., Kemerink, G.J., Bouvy, N.D., et al., 2009. Cold-activated brown adipose tissue in healthy men. *The New England Journal of Medicine* 360:1500–1508.
- [5] Virtanen, K.A., Lidell, M.E., Orava, J., Heglind, M., Westergren, R., Niemi, T., et al., 2009. Functional brown adipose tissue in healthy adults. *The New England Journal of Medicine* 360:1518–1525.
- [6] Schrauwen, P., van Marken Lichtenbelt, W.D., Spiegelman, B.M., 2015. The future of brown adipose tissues in the treatment of type 2 diabetes. *Diabetologia* 58:1704–1707.
- [7] Barbatelli, G., Murano, I., Madsen, L., Hao, Q., Jimenez, M., Kristiansen, K., et al., 2010. The emergence of cold-induced brown adipocytes in mouse white fat depots is determined predominantly by white to brown adipocyte trans-differentiation. *American Journal of Physiology. Endocrinology and Metabolism* 298:E1244–E1253.
- [8] Cousin, B., Cinti, S., Morrioni, M., Raimbault, S., Ricquier, D., Penicaud, L., et al., 1992. Occurrence of brown adipocytes in rat white adipose tissue: molecular and morphological characterization. *Journal of Cell Science* 103(Pt 4):931–942.
- [9] Young, P., Arch, J.R., Ashwell, M., 1984. Brown adipose tissue in the parametrial fat pad of the mouse. *FEBS Letters* 167:10–14.
- [10] Guerra, C., Koza, R.A., Yamashita, H., Walsh, K., Kozak, L.P., 1998. Emergence of brown adipocytes in white fat in mice is under genetic control. Effects on body weight and adiposity. *Journal of Clinical Investigation* 102:412–420.
- [11] Himms-Hagen, J., Melnyk, A., Zingaretti, M.C., Ceresi, E., Barbatelli, G., Cinti, S., 2000. Multilocular fat cells in WAT of CL-316243-treated rats derive directly from white adipocytes. *American Journal of Physiology. Cell Physiology* 279:C670–C681.
- [12] Nagase, I., Yoshida, T., Kumamoto, K., Umekawa, T., Sakane, N., Nikami, H., et al., 1996. Expression of uncoupling protein in skeletal muscle and white fat of obese mice treated with thermogenic beta 3-adrenergic agonist. *Journal of Clinical Investigation* 97:2898–2904.
- [13] Rosell, M., Kafrou, M., Frontini, A., Okolo, A., Chan, Y.W., Nikolopoulou, E., et al., 2014. Brown and white adipose tissues: intrinsic differences in gene expression and response to cold exposure in mice. *American Journal of Physiology. Endocrinology and Metabolism* 306:E945–E964.
- [14] Walden, T.B., Hansen, I.R., Timmons, J.A., Cannon, B., Nedergaard, J., 2012. Recruited vs. nonrecruited molecular signatures of brown, “brite,” and white adipose tissues. *American Journal of Physiology. Endocrinology and Metabolism* 302:E19–E31.
- [15] Frontini, A., Cinti, S., 2010. Distribution and development of brown adipocytes in the murine and human adipose organ. *Cell Metabolism* 11:253–256.
- [16] Cohen, P., Levy, J.D., Zhang, Y., Frontini, A., Kolodin, D.P., Svensson, K.J., et al., 2014. Ablation of PRDM16 and beige adipose causes metabolic dysfunction and a subcutaneous to visceral fat switch. *Cell* 156:304–316.
- [17] Seale, P., Conroe, H.M., Estall, J., Kajimura, S., Frontini, A., Ishibashi, J., et al., 2011. Prdm16 determines the thermogenic program of subcutaneous white adipose tissue in mice. *Journal of Clinical Investigation* 121:96–105.
- [18] Wang, Q.A., Tao, C., Gupta, R.K., Scherer, P.E., 2013. Tracking adipogenesis during white adipose tissue development, expansion and regeneration. *Nature Medicine* 19:1338–1344.
- [19] Wu, J., Bostrom, P., Sparks, L.M., Ye, L., Choi, J.H., Giang, A.H., et al., 2012. Beige adipocytes are a distinct type of thermogenic fat cell in mouse and human. *Cell* 150:366–376.
- [20] Lee, Y.H., Petkova, A.P., Konkar, A.A., Granneman, J.G., 2015. Cellular origins of cold-induced brown adipocytes in adult mice. *FASEB Journal* 29:286–299.
- [21] Rosenwald, M., Perdikari, A., Rulicke, T., Wolfrum, C., 2013. Bi-directional interconversion of brite and white adipocytes. *Nature Cell Biology* 15:659–667.
- [22] Frontini, A., Vitali, A., Perugini, J., Murano, I., Romiti, C., Ricquier, D., et al., 2013. White-to-brown transdifferentiation of omental adipocytes in patients

- affected by pheochromocytoma. *Biochimica et Biophysica Acta* 1831:950–959.
- [23] Sidossis, L.S., Porter, C., Saraf, M.K., Borsheim, E., Radhakrishnan, R.S., Chao, T., et al., 2015. Browning of subcutaneous white adipose tissue in humans after severe adrenergic stress. *Cell Metabolism* 22:219–227.
- [24] Ahfeldt, T., Schinzel, R.T., Lee, Y.K., Hendrickson, D., Kaplan, A., Lum, D.H., et al., 2012. Programming human pluripotent stem cells into white and brown adipocytes. *Nature Cell Biology* 14:209–219.
- [25] Boulet, N., Esteve, D., Bouloumie, A., Galitzky, J., 2013. Cellular heterogeneity in superficial and deep subcutaneous adipose tissues in overweight patients. *Journal of Physiology and Biochemistry* 69:575–583.
- [26] Lee, J.Y., Hashizaki, H., Goto, T., Sakamoto, T., Takahashi, N., Kawada, T., 2011. Activation of peroxisome proliferator-activated receptor- $\alpha$  enhances fatty acid oxidation in human adipocytes. *Biochemical and Biophysical Research Communications* 407:818–822.
- [27] Shinoda, K., Luijten, I.H., Hasegawa, Y., Hong, H., Sonne, S.B., Kim, M., et al., 2015. Genetic and functional characterization of clonally derived adult human brown adipocytes. *Nature Medicine* 21:389–394.
- [28] Xue, R., Lynes, M.D., Dreyfuss, J.M., Shamsi, F., Schulz, T.J., Zhang, H., et al., 2015. Clonal analyses and gene profiling identify genetic biomarkers of the thermogenic potential of human brown and white preadipocytes. *Nature Medicine* 21:760–768.
- [29] Elabd, C., Chiellini, C., Carmona, M., Galitzky, J., Cochet, O., Petersen, R., et al., 2009. Human multipotent adipose-derived stem cells differentiate into functional brown adipocytes. *Stem Cells* 27:2753–2760.
- [30] Loft, A., Fors, I., Siersbaek, M.S., Schmidt, S.F., Larsen, A.S., Madsen, J.G., et al., 2015. Browning of human adipocytes requires KLF11 and reprogramming of PPAR $\gamma$  superenhancers. *Genes & Development* 29:7–22.
- [31] Pisani, D.F., Djedaini, M., Beranger, G.E., Elabd, C., Scheideler, M., Ailhaud, G., et al., 2011. Differentiation of human adipose-derived stem cells into “brite” (brown-in-white) adipocytes. *Frontiers in Endocrinology (Lausanne)* 2:87.
- [32] Hondares, E., Rosell, M., Diaz-Delfin, J., Olmos, Y., Monsalve, M., Iglesias, R., et al., 2011. Peroxisome proliferator-activated receptor  $\alpha$  (PPAR $\alpha$ ) induces PPAR $\gamma$  coactivator 1 $\alpha$  (PGC-1 $\alpha$ ) gene expression and contributes to thermogenic activation of brown fat: involvement of PRDM16. *Journal of Biological Chemistry* 286:43112–43122.
- [33] Rachid, T.L., Penna-de-Carvalho, A., Bringham, I., Aguilu, M.B., Mandarim-de-Lacerda, C.A., Souza-Mello, V., 2015. Fenofibrate (PPAR $\alpha$  agonist) induces beige cell formation in subcutaneous white adipose tissue from diet-induced male obese mice. *Molecular and Cellular Endocrinology* 402:86–94.
- [34] Hondares, E., Mora, O., Yubero, P., Rodriguez de la Concepcion, M., Iglesias, R., Giralt, M., et al., 2006. Thiazolidinediones and rexinoids induce peroxisome proliferator-activated receptor-coactivator (PGC)-1 $\alpha$  gene transcription: an autoregulatory loop controls PGC-1 $\alpha$  expression in adipocytes via peroxisome proliferator-activated receptor- $\gamma$  coactivation. *Endocrinology* 147:2829–2838.
- [35] Petrovic, N., Walden, T.B., Shabalina, I.G., Timmons, J.A., Cannon, B., Nedergaard, J., 2010. Chronic peroxisome proliferator-activated receptor  $\gamma$  (PPAR $\gamma$ ) activation of epididymally derived white adipocyte cultures reveals a population of thermogenically competent, UCP1-containing adipocytes molecularly distinct from classic brown adipocytes. *Journal of Biological Chemistry* 285:7153–7164.
- [36] Pisani, D.F., Ghandour, R.A., Beranger, G.E., Le Faouder, P., Chambard, J.C., Giroud, M., et al., 2014. The omega6-fatty acid, arachidonic acid, regulates the conversion of white to brite adipocyte through a prostaglandin/calcium mediated pathway. *Molecular Metabolism* 3:834–847.
- [37] Brown, P.J., Stuart, L.W., Hurley, K.P., Lewis, M.C., Winegar, D.A., Wilson, J.G., et al., 2001. Identification of a subtype selective human PPAR- $\alpha$  agonist through parallel-array synthesis. *Bioorganic & Medicinal Chemistry Letters* 11:1225–1227.
- [38] Seimandi, M., Lemaire, G., Pillon, A., Perrin, A., Carlván, I., Voegel, J.J., et al., 2005. Differential responses of PPAR $\alpha$ , PPAR $\delta$ , and PPAR $\gamma$  reporter cell lines to selective PPAR synthetic ligands. *Analytical Biochemistry* 344:8–15.
- [39] Klimcakova, E., Roussel, B., Marquez-Quinones, A., Kovacova, Z., Kovacikova, M., Combes, M., et al., 2011. Worsening of obesity and metabolic status yields similar molecular adaptations in human subcutaneous and visceral adipose tissue: decreased metabolism and increased immune response. *The Journal of Clinical Endocrinology & Metabolism* 96: E73–E82.
- [40] Huang da, W., Sherman, B.T., Lempicki, R.A., 2009. Systematic and integrative analysis of large gene lists using DAVID bioinformatics resources. *Nature Protocols* 4:44–57.
- [41] Ribet, C., Montastier, E., Valle, C., Bezaire, V., Mazzucotelli, A., Mairal, A., et al., 2010. Peroxisome proliferator-activated receptor- $\alpha$  control of lipid and glucose metabolism in human white adipocytes. *Endocrinology* 151:123–133.
- [42] Bezaire, V., Mairal, A., Ribet, C., Lefort, C., Grousse, A., Jocken, J., et al., 2009. Contribution of adipose triglyceride lipase and hormone-sensitive lipase to lipolysis in hMADS adipocytes. *Journal of Biological Chemistry* 284:18282–18291.
- [43] Grousse, A., Tavernier, G., Valle, C., Moro, C., Mejhert, N., Dinel, A.L., et al., 2013. Partial inhibition of adipose tissue lipolysis improves glucose metabolism and insulin sensitivity without alteration of fat mass. *PLOS Biology* 11: e1001485.
- [44] Montagner, A., Polizzi, A., Fouche, E., Ducheix, S., Lippi, Y., Lasserre, F., et al., 2016. Liver PPAR $\alpha$  is crucial for whole-body fatty acid homeostasis and is protective against NAFLD. *Gut*.
- [45] Cypess, A.M., White, A.P., Vernochet, C., Schulz, T.J., Xue, R., Sass, C.A., et al., 2013. Anatomical localization, gene expression profiling and functional characterization of adult human neck brown fat. *Nature Medicine* 19:635–639.
- [46] Jespersen, N.Z., Larsen, T.J., Peijs, L., Dagaard, S., Homoe, P., Loft, A., et al., 2013. A classical brown adipose tissue mRNA signature partly overlaps with brite in the supraclavicular region of adult humans. *Cell Metabolism* 17: 798–805.
- [47] Lidell, M.E., Betz, M.J., Dahlqvist Leinhard, O., Heglund, M., Elander, L., Slawik, M., et al., 2013. Evidence for two types of brown adipose tissue in humans. *Nature Medicine* 19:631–634.
- [48] Sharp, L.Z., Shinoda, K., Ohno, H., Scheel, D.W., Tomoda, E., Ruiz, L., et al., 2012. Human BAT possesses molecular signatures that resemble beige/brite cells. *PLOS One* 7:e49452.
- [49] Nedergaard, J., Cannon, B., 2013. How brown is brown fat? It depends where you look. *Nature Medicine* 19:540–541.
- [50] Christodoulides, C., Vidal-Puig, A., 2010. PPARs and adipocyte function. *Molecular and Cellular Endocrinology* 318:61–68.
- [51] Bostrom, P., Wu, J., Jedrychowski, M.P., Korde, A., Ye, L., Lo, J.C., et al., 2012. A PGC1- $\alpha$ -dependent myokine that drives brown-fat-like development of white fat and thermogenesis. *Nature* 481:463–468.
- [52] Roberts, L.D., Bostrom, P., O’Sullivan, J.F., Schinzel, R.T., Lewis, G.D., Dejam, A., et al., 2014. beta-Aminoisobutyric acid induces browning of white fat and hepatic beta-oxidation and is inversely correlated with cardiometabolic risk factors. *Cell Metabolism* 19:96–108.
- [53] Kersten, S., Seydoux, J., Peters, J.M., Gonzalez, F.J., Desvergne, B., Wahli, W., 1999. Peroxisome proliferator-activated receptor  $\alpha$  mediates the adaptive response to fasting. *Journal of Clinical Investigation* 103:1489–1498.
- [54] Beranger, G.E., Karbiener, M., Barquissau, V., Pisani, D.F., Scheideler, M., Langin, D., et al., 2013. In vitro brown and “brite”/“beige” adipogenesis: human cellular models and molecular aspects. *Biochimica et Biophysica Acta* 1831:905–914.

- [55] Gburcik, V., Cleasby, M.E., Timmons, J.A., 2013. Loss of neuronatin promotes “browning” of primary mouse adipocytes while reducing Glut1-mediated glucose disposal. *American Journal of Physiology. Endocrinology and Metabolism* 304:E885–E894.
- [56] Mossenbock, K., Vegiopoulos, A., Rose, A.J., Sijmonsma, T.P., Herzig, S., Schafmeier, T., 2014. Browning of white adipose tissue uncouples glucose uptake from insulin signaling. *PLOS One* 9:e110428.
- [57] Komatsu, M., Tong, Y., Li, Y., Nakajima, T., Li, G., Hu, R., et al., 2010. Multiple roles of PPARalpha in brown adipose tissue under constitutive and cold conditions. *Genes Cells* 15:91–100.
- [58] Hao, Q., Yadav, R., Basse, A.L., Petersen, S., Sonne, S.B., Rasmussen, S., et al., 2015. Transcriptome profiling of brown adipose tissue during cold exposure reveals extensive regulation of glucose metabolism. *American Journal of Physiology. Endocrinology and Metabolism* 308:E380–E392.
- [59] Labbe, S.M., Caron, A., Bakan, I., Laplante, M., Carpentier, A.C., Lecomte, R., et al., 2015. In vivo measurement of energy substrate contribution to cold-induced brown adipose tissue thermogenesis. *FASEB Journal* 29:2046–2058.
- [60] Cadoudal, T., Distel, E., Durant, S., Fouque, F., Blouin, J.M., Collinet, M., et al., 2008. Pyruvate dehydrogenase kinase 4: regulation by thiazolidinediones and implication in glyceroneogenesis in adipose tissue. *Diabetes* 57:2272–2279.
- [61] Nye, C., Kim, J., Kalhan, S.C., Hanson, R.W., 2008. Reassessing triglyceride synthesis in adipose tissue. *Trends in Endocrinology and Metabolism* 19:356–361.
- [62] Patsouris, D., Mandard, S., Voshol, P.J., Escher, P., Tan, N.S., Havekes, L.M., et al., 2004. PPARalpha governs glycerol metabolism. *Journal of Clinical Investigation* 114:94–103.
- [63] Guan, H.P., Li, Y., Jensen, M.V., Newgard, C.B., Steppan, C.M., Lazar, M.A., 2002. A futile metabolic cycle activated in adipocytes by antidiabetic agents. *Nature Medicine* 8:1122–1128.
- [64] Mazzucotelli, A., Viguierie, N., Tiraby, C., Annicotte, J.S., Mairal, A., Klimcakova, E., et al., 2007. The transcriptional coactivator peroxisome proliferator activated receptor (PPAR)gamma coactivator-1 alpha and the nuclear receptor PPAR alpha control the expression of glycerol kinase and metabolism genes independently of PPAR gamma activation in human white adipocytes. *Diabetes* 56:2467–2475.
- [65] Berbee, J.F., Boon, M.R., Khedoe, P.P., Bartelt, A., Schlein, C., Worthmann, A., et al., 2015. Brown fat activation reduces hypercholesterolaemia and protects from atherosclerosis development. *Nature Communications* 6:6356.
- [66] Baba, S., Jacene, H.A., Engles, J.M., Honda, H., Wahl, R.L., 2010. CT Hounsfield units of brown adipose tissue increase with activation: preclinical and clinical studies. *Journal of Nuclear Medicine* 51:246–250.
- [67] Ouellet, V., Labbe, S.M., Blondin, D.P., Phoenix, S., Guerin, B., Haman, F., et al., 2012. Brown adipose tissue oxidative metabolism contributes to energy expenditure during acute cold exposure in humans. *Journal of Clinical Investigation* 122:545–552.
- [68] Blondin, D.P., Labbe, S.M., Noll, C., Kunach, M., Phoenix, S., Guerin, B., et al., 2015. Selective impairment of glucose but not fatty acid or oxidative metabolism in brown adipose tissue of subjects with type 2 diabetes. *Diabetes* 64: 2388–2397.